

Article

Optimal Low-Carbon Economic Environmental Dispatch of Hybrid Electricity-Natural Gas Energy Systems Considering P2G

Jing Liu ^{1,*}, Wei Sun ²  and Gareth P. Harrison ² 

¹ School of Mechanical Electronic and Information Engineering, China University of Mining & Technology (Beijing), Beijing 100083, China

² School of Engineering, University of Edinburgh, Edinburgh EH9 3DW, UK; W.Sun@ed.ac.uk (W.S.); Gareth.Harrison@ed.ac.uk (G.P.H.)

* Correspondence: jingqisandra@163.com; Tel.: +86-010-6233-1180

Received: 8 March 2019; Accepted: 5 April 2019; Published: 9 April 2019



Abstract: Power to gas facilities (P2G) could absorb excess renewable energy that would otherwise be curtailed due to electricity network constraints by converting it to methane (synthetic natural gas). The produced synthetic natural gas can power gas turbines and realize bidirectional energy flow between power and natural-gas systems. P2G, therefore, has significant potential for unlocking inherent flexibility in the integrated system, but also poses new challenges of increased system complexity. A coordinated operation strategy that manages power and natural-gas network constraints together is essential to address such challenges. In this paper, a novel low-carbon economic environmental dispatch strategy is presented considering all the constraints in both systems. The multi-objective black-hole particle swarm optimization algorithm (MOBHPSO) is adopted. In addition to P2G, a gas demand management strategy is proposed to support gas flow balance. A new solving approach that combines the effective redundancy method, trust region method, and Levenberg-Marquardt method is proposed to address the complex coupled constraints. Case studies that use an integrated IEEE 39-bus power and Belgian high-calorific 20-node gas system demonstrate the effectiveness and scalability of the proposed model and optimization method. The analysis of dispatch results illustrates the benefit of P2G for the wind power accommodation, and low-carbon, economic, and environmental improvement of integrated system operation.

Keywords: hybrid electricity-natural gas energy systems; power to gas (P2G); low-carbon; economic environmental dispatch; trust region method; Levenberg-Marquardt method

1. Introduction

With further acceleration of the low-carbon energy process, as well as the energy crisis, environmental pollution, and other issues, the capacity of renewable energy sources has increased continuously. Due to the intermittency and uncertainty of wind power as well as the lack of peak load regulation of power system, it is likely that more and more wind power generation will have to be curtailed in order to maintain the power system reliability [1]. To solve this problem, much research is carried out to explore practical means to reduce the curtailment of wind power generation. The growing interdependence of the power system and natural-gas system and the development of power to gas technologies [2–8] creates operational interactions between the power system and natural-gas system, which could obtain additional benefits for both systems, including reducing the curtailed wind power generation. On the one hand, the power system tends to require more flexible power energy from the natural-gas system to shift peak load compared with the gas-fired units [3],

which is conducive to the accommodation of wind power. On the other hand, the natural-gas system absorbs methane or hydrogen produced by P2G to guarantee the continuity of gas supply and the wind power energy will be stored and transported in the existing natural-gas system for generating low-carbon electricity or heat later [9–11], which uses the curtailed wind power directly. Therefore, the integrated electricity-natural gas energy systems with P2G have become one of the effective forms to reduce the curtailment of wind power generation.

The diagram of integrated electricity-natural gas energy systems with P2G is shown in Figure 1. It can be seen that the power system and the natural-gas system exchange the energy between P2G and gas-fired units. When the curtailed wind power is converted to hydrogen or methane through power to hydrogen facilities (P2H) or power to methane facilities (P2M), P2G which includes P2H and P2M is the load of power system and the gas source of natural-gas system. Meanwhile, the gas-fired units are the load of natural-gas system and the generators of power system. Obviously, operation parameters of P2G, power system and natural-gas system are interrelated and interactive which can affect the operation cost, CO₂ emissions, reliability, and stability of both systems. Therefore, how to deal with the interactive relationship between power system and natural-gas system and how to achieve coordinated optimal operation with economic environmental benefits are the key issues for the integrated power system and natural-gas system.

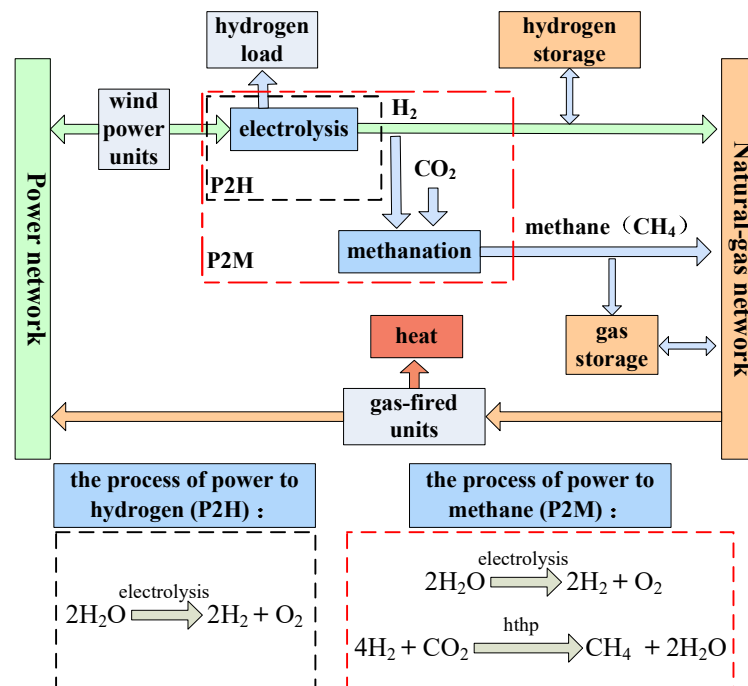


Figure 1. Diagram of integrated electricity and natural-gas energy systems with power to gas (P2G).

For the integrated electricity-natural gas energy systems, the initial research is focused on optimal power flow [12–15], unit commitment [16], optimal dispatch [17–19], steady-state analysis [20], and system planning [21]. For the calculation of optimal power flow, the total operation cost is usually considered as optimal objective and the dual interior point method [12], the Monte Carlo method [13] and the point estimation method [14] are adopted frequently. Some studies introduce an energy hub to deal with the translation of different energies in the hybrid electricity-natural gas energy systems [13,17]. For the optimization of system operation, the operation of power system and the operation of natural-gas system are mostly optimized separately using the deterministic optimization methods or stochastic optimization methods [18]. For the steady-state analysis of the hybrid electricity-natural gas energy systems, based on the steady-state analysis of power system, the analysis model of natural-gas system is realized by analogy analysis between power system and natural-gas system, and then

the comprehensive steady-state analysis model of hybrid electricity-natural gas energy systems is given [20]. For the optimal system planning, a chance constrained programming approach is presented to minimize the investment cost of the integrated energy systems [21]. In these studies, P2G is not considered. As the coupling operation link of the power system and natural-gas system, P2G plays a more and more important role in wind power accommodation with broad prospects and potential for energy development [22–24]. Therefore, it is necessary to carry out the research on optimal operation of integrated electricity-natural gas energy systems considering P2G. The early studies on P2G are mainly focused on technology implementation and security application [6,25–28]. Recently, although some achievements about optimal operation of integrated electricity-natural gas energy systems considering P2G have been achieved [6–8,24,29–38], it still seems to be in the exploratory stage from the following aspects.

(1) Optimal objectives: The minimum total operation cost is mostly adopted [6,24,29–32,37]. In only a few studies, the maximum wind power accommodation [33], the minimum energy purchase cost [34], or net power demand smoothness [38] is also considered as the objective. However, environmental benefit is rarely considered. As we know, the low-carbon and emission reduction requirements become more and more important. Therefore, it is necessary to take environmental benefit into consideration.

(2) Optimal models: The operation model of power system and operation model of natural-gas system are mainly established separately based on the two-level optimal power flow structure [6,30–32]. It seems that rare consideration is given to coordinated optimization between the two energy systems.

(3) Optimal algorithms: Generally, the traditional algorithms are adopted in most studies, such as the mix-integer linear programming method [3,24], mixed-integer quadratic programming method [37], and interior point method [35]. However, the intelligent optimization algorithms with high global search ability and fast convergence speed are rarely used.

(4) Constraints handling methods: The constraints handling methods affect the operation results directly. Few articles give full details about the constraints handling methods, especially for the complicated dynamic nodal balance constraint and volume limits of gas storage in the natural-gas system.

On the above premises, this paper establishes the optimal operation model of the hybrid electricity-natural gas energy systems considering operation cost, natural-gas cost reduction due to P2G, CO₂ emissions, and SO_x emissions to achieve low-carbon, economic, and environmental benefits. The multi-objective black-hole particle swarm optimization algorithm (MOBHPSO) [39–42] is adopted. The power flow is calculated using the Newton-Raphson method. The non-linear gas flow equations are solved by the trust region method [43,44] and Levenberg-Marquardt (L-M) method [45,46], respectively. The gas demand management strategy is proposed to balance the gas flow. Moreover, the detailed handling methods of inequality constraints in natural-gas system are also given in this paper. Several case studies are carried out on a hybrid IEEE 39-bus power system and Belgian high-calorific 20-node gas system in a period of 24 h to investigate the low-carbon, economic and environmental benefits of P2G in terms of cost reduction ($\$6.165 \times 10^5$), rate decline of wind curtailment (from 24.85% to 4.04%), CO₂ emissions reduction (3630 tons), and SO_x emissions reduction (0.254 ton).

2. Problem Formulation

The optimal low-carbon economic environmental dispatch problem of hybrid electricity-natural gas energy systems with P2G is a complicated non-convex, coupled, non-linear, multi-objective, and multi-constraint optimization problem. It contains three parts: The first one is the optimization of power system; the second one is the optimization of natural-gas system; and the last one is the coordination of the hybrid electricity-natural gas energy systems. The flow chart of this optimization problem is shown in Figure 2. Each part of the flow chart will be described in detail.

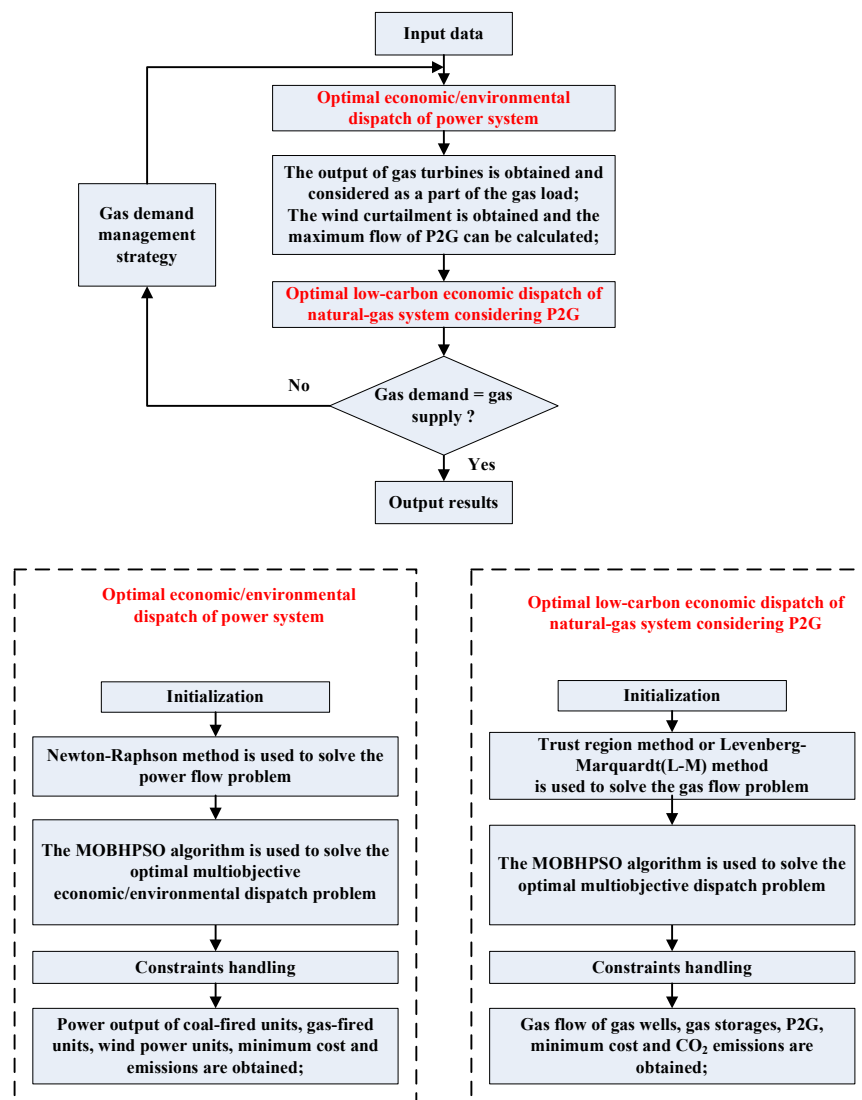


Figure 2. Flow chart.

2.1. Optimal Economic Environmental Dispatch of Power System

2.1.1. Objectives

- (1) Minimum Fuel Cost of the Power System

$$\text{Min } F_p = \sum_{i=1}^{N_G} \sum_{t=1}^T a_i P_{Gi}(t)^2 + b_i P_{Gi}(t) + c_i \tag{1}$$

- (2) Minimum SO_x Pollutant Emissions of the Power System

$$\text{Min } E_{SO_x} = \sum_{i=1}^{N_G} \sum_{t=1}^T (\alpha_i + \beta_i P_{Gi}(t) + \gamma_i P_{Gi}(t)^2 + \delta_i e^{\lambda_i P_{Gi}(t)}) \tag{2}$$

- (3) Minimum Load Loss Rate of the Power System

$$\text{Min } L_p = \frac{\sum_{t=1}^T \left[P_L(t) + \sum_{k=1}^{N_{P2G}} P_{P2G,k}(t) - \sum_{i=1}^{N_G} P_{Gi}(t) \right]}{\sum_{t=1}^T P_L(t)} \tag{3}$$

where F_p is the fuel cost of power system; N_G is the number of power generations; T is the number of time periods; $P_{Gi}(t)$ is the power generation output at time t ; a_i, b_i, c_i are coefficient of the fuel cost;

E_{SO_x} is the pollutant emission of SO_x ; $\alpha_i, \beta_i, \gamma_i, \delta_i, \lambda_i$ are coefficient of the pollutant emission; L_p is the load loss rate presenting the reliability of power supply; N_{P2G} is the number of P2G; $P_L(t)$ is the power load at time t ; $P_{P2G}(t)$ is the power supplied to the P2G facilities at time t .

The power output of gas-fired units is calculated by the product of the gas flow injected to the gas-fired units $Q_{GT}(t)$, higher heating value of natural gas HHV_g and the energy conversion efficiency $\eta_{GT}(t)$. In this paper, the last objective is converted into a constraint by being less than a given value ε .

2.1.2. Constraints

(1) Power Output Limits

$$P_{Gi}^{\min} \leq P_{Gi}(t) \leq P_{Gi}^{\max} \quad (4)$$

where P_{Gi}^{\min} and P_{Gi}^{\max} represent the minimum power output and maximum power output of unit i , respectively.

(2) Ramp Rate Limits

$$\begin{cases} P_{Gi}(t) \geq \max\{P_{Gi}^{\min}, P_{Gi}(t-1) - \Delta P_{Gi}^{\text{down}}\}, & P_{Gi}(t) \leq P_{Gi}(t-1) \\ P_{Gi}(t) \leq \min\{P_{Gi}^{\max}, P_{Gi}(t-1) + \Delta P_{Gi}^{\text{up}}\}, & P_{Gi}(t) \geq P_{Gi}(t-1) \end{cases} \quad (5)$$

where $\Delta P_{Gi}^{\text{up}}$ and $\Delta P_{Gi}^{\text{down}}$ represent the ramp up rate and the ramp down rate of unit i , respectively.

(3) Line Capacity Limit

$$S_l(t) \leq S_l^{\max} \quad (6)$$

where S_l^{\max} is the maximum capacity of line l .

2.2. Optimal Low-Carbon Economic Dispatch of Natural-Gas System Considering P2G

2.2.1. Objectives

(1) Minimum the Operational Cost of Natural-Gas System

$$\text{Min } C_{well} + C_{gs} + C_{P2G} - S_{P2G} \quad (7)$$

$$C_{well} = \sum_{n=1}^{N_w} \sum_{t=1}^T Q_{wn}(t) u_{wn}(t) \quad (8)$$

$$C_{gs} = \sum_{m=1}^{N_{gs}} \sum_{t=1}^T Q_{gs,m}(t) u_{gs,m}(t) \quad (9)$$

$$C_{P2G} = \sum_{k=1}^{N_{P2G}} \sum_{t=1}^T P_{P2G,k}(t) u_{P2G,k} \quad (10)$$

$$S_{P2G} = \sum_{k=1}^{N_{P2G}} \sum_{t=1}^T Q_{P2G,k}(t) u_{ave}(t) \quad (11)$$

where C_{well} , C_{gs} , and C_{P2G} represent the operation cost of gas wells, the operation cost of gas storage, and the operation cost of P2G, respectively. S_{P2G} is the saved natural-gas cost due to the P2G. N_w , N_{gs} represent the number of gas wells and the number of gas storage, respectively; $Q_{wn}(t)$ is the gas flow of gas well n ; $u_{wn}(t)$ is the gas price of gas well n at time t ; $Q_{gs,m}(t)$ is the gas flow of gas storage m at time t (It is positive for inflow and negative for outflow); $u_{gs,m}(t)$ is the storage price for gas storage m at time t ; $u_{P2G,k}$ is the operation cost of P2G k ; $Q_{P2G,k}(t)$ is the gas flow of P2G k at time t ; $u_{ave}(t)$ is the average gas price (In this paper, it is the average price of gas wells).

(2) Minimum CO₂ Emissions of the Natural-Gas System

$$\text{Min } E_{CO_2} = \sum_{n=1}^{N_w} \sum_{t=1}^T E_{wn}(t) + \sum_{m=1}^{N_{gs}} \sum_{t=1}^T E_{gs,m}(t) - \sum_{k=1}^{N_{P2G}} \sum_{t=1}^T E_{P2G,k}(t) \quad (12)$$

where E_{CO_2} represents CO₂ emissions of the natural-gas system; $E_{wn}(t)$, $E_{gs,m}(t)$ are the CO₂ emissions of gas well n , gas storage m at time t , respectively; $E_{P2G,k}(t)$ is the amount of CO₂ absorbed by the methanation process of P2G k at time t .

2.2.2. Constraints

(1) Gas Flow Limits of Gas Wells

$$Q_{wn}^{\min} \leq Q_{wn}(t) \leq Q_{wn}^{\max} \quad (13)$$

where Q_{wn}^{\min} , Q_{wn}^{\max} represent the minimum gas flow and the maximum gas flow of gas well n , respectively.

(2) Gas Pressure Limits of Gas Nodes

$$M_i^{\min} \leq M_i(t) \leq M_i^{\max} \quad (14)$$

where $M_i(t)$ represents gas pressure of gas node i at time t . M_i^{\min} and M_i^{\max} are the minimum and maximum gas pressure of gas node i .

(3) Gas Flow Equation of Pipelines

The natural-gas system satisfies the mass conservation law of fluid dynamics and Bernoulli equation in the operation. The relationship between gas flow of pipelines and gas pressure of gas nodes can be modeled as follows [12,35].

$$Q_{ij}(t)|Q_{ij}(t)| = C_{ij}(M_i(t)^2 - M_j(t)^2) \quad (15)$$

$$Q_{ij}(t) = \frac{Q_{ij}^{in}(t) + Q_{ij}^{out}(t)}{2} \quad (16)$$

where $Q_{ij}(t)$ is the average gas flow of pipeline ij (Pipeline ij is the pipeline between gas node i and gas node j); $Q_{ij}^{in}(t)$ and $Q_{ij}^{out}(t)$ are the injection and withdrawal gas flow of pipeline ij , respectively; C_{ij} is a constant related to the length, diameter, temperature and compressibility factor of pipeline ij .

(4) Line Pack Equation

Due to the compressibility of natural gas, the injection gas flow and the withdrawal gas flow of the same pipeline would be different. Some excess natural gas can be stored in the pipelines, which is called line pack. The line pack of pipeline ij is related to the average pressure and its own parameters of pipelines, which can be modeled as below [12,15].

$$L_{ij}(t) = \omega_{ij}M_{ij}(t) \quad (17)$$

$$M_{ij}(t) = \frac{M_i(t) + M_j(t)}{2} \quad (18)$$

$$L_{ij}(t) = L_{ij}(t-1) + Q_{ij}^{in}(t) - Q_{ij}^{out}(t) \quad (19)$$

where $L_{ij}(t)$ is the line pack of pipeline ij at time t ; ω_{ij} is a constant related to pipeline parameters, gas constant, compressibility factor, gas density, and gas temperature.

(5) Nodal Gas Flow Balance Equation

For each gas node, the gas flows into the node must equals the gas flows out of the node.

$$\begin{aligned} & \sum_{n \in i} Q_{wn}(t) + \sum_{m \in i} Q_{gs,m}(t) + \sum_{k \in i} Q_{P2G,k}(t) - \sum_{j \in Set_I(i)} Q_{ij}^{in}(t) \\ & + \sum_{j \in Set_O(i)} Q_{ij}^{out}(t) - Q_{GT,i}(t) - Q_{Li}(t) = 0 \end{aligned} \quad (20)$$

where, the first three items are the gas flow of gas wells, gas storage, and P2G located at gas node i at time t , respectively; $Q_{GT,i}(t)$ and $Q_{Li}(t)$ indicate the gas flow injected to gas-fired units and the gas load at gas node i at time t , respectively; $Set_I(i)$ is the set of pipeline ij which lets gas node i as the input node; $Set_O(i)$ is the set of pipeline ij which lets gas node i as the output node.

(6) Gas Flow Limits and Capacity Limits of Gas Storage

$$Q_{gs,m}^{\min} \leq Q_{gs,m}(t) \leq Q_{gs,m}^{\max} \quad (21)$$

$$V_m^{\min} \leq V_m(t) \leq V_m^{\max} \quad (22)$$

$$V_m(t) = V_m(t-1) + Q_{gs,m}(t) \quad (23)$$

where $Q_{gs,m}^{\min}$ and $Q_{gs,m}^{\max}$ are the minimum and maximum gas flow of gas storage m , respectively; $V_m(t)$, V_m^{\min} , V_m^{\max} are the capacity of gas storage m at time t , the minimum and maximum capacity of gas storage m , respectively. When the gas is injected to the gas storage, $Q_{gs,m}(t)$ is positive, otherwise it is negative.

(7) Compressor

The compressors are used to boost the pressure of the natural-gas network, which can help the natural gas transporting to each gas load. In this paper, the energy consumed by the compressors is calculated by using natural gas flow through the compressors. The consumed gas flow of compressor r , $Q_{cr}^{consume}(t)$, is calculated as presented below [15].

$$Q_{cr}^{consume}(t) = \beta_{cr} P_{cr}(t) \quad (24)$$

$$P_{cr}(t) = \frac{Q_{cr}(t)}{\eta_{cr} \cdot \tau} \cdot \left(\left(\frac{M_{or}(t)}{M_{ir}(t)} \right)^{\tau} - 1 \right) \quad (25)$$

where β_{cr} is energy conversion coefficient of compressor r ; $P_{cr}(t)$ is the consumed energy by compressor r ; $Q_{cr}(t)$ is the gas flow flowing through compressor r at time t ; η_{cr} is the efficiency of compressor r ; $\tau = (\alpha - 1)/\alpha$ and α is variability index of compressors; $M_{or}(t)$ and $M_{ir}(t)$ are the pressure of output node and input node of compressor r , respectively.

(8) Gas Flow Limit of P2G

$$Q_{P2G,k}^{\min} \leq Q_{P2G,k}(t) \leq Q_{P2G,k}^{\max} \quad (26)$$

where $Q_{P2G,k}^{\min}$ and $Q_{P2G,k}^{\max}$ are the minimum and maximum gas flow of P2G k , respectively.

2.3. Gas Demand Management Strategy to Coordinate the Two Energy Systems

When the pressure of some gas nodes is higher than the maximum pressure or lower than the minimum pressure, which means the gas demand and the gas supply is not balanced on these gas nodes, then the gas demand management strategy is used. The main idea is to adjust the gas flow of gas turbines to achieve the gas demand balance, which means changing the power output of gas-fired units. Then, the power output of units in power system will be adjusted.

2.4. Constraints Handling Methods

The constraints of power system are handled using the methods presented in Reference [39]. In this paper, the constraints of natural-gas system are handled by the proposed method as shown below.

2.4.1. Equality Constraints Handling Method

In this paper, the set of non-linear constraints Equations (15)–(20) of the natural-gas system are solved by the trust region algorithm [43,44] and Levenberg-Marquardt algorithm (L-M) [45,46]. Trust region and L-M methods are both simple and powerful tools for solving systems of nonlinear equations and large-scale optimization problems. They have the advantages of guaranteeing a solution whenever it exists [43–46]. In this paper, the trust region method and L-M method are used to solve the gas flow non-linear equations, respectively. The optimization results are compared in the case studies.

2.4.2. Inequality Constraints Handling Method

For the inequality constraints (13)–(14), (21)–(22), (26), the gas flow is the minimum when it is lower than the minimum value and the gas flow is the maximum when it is over the maximum value. For the gas storage volume constraint, the effective redundancy method is proposed in this paper. The details of this method are as below.

- a) For gas storage m at time t ;
- b) If $V_m(t) \leq V_m^{min}$, calculate $\Delta V = V_m^{min} - V_m(t)$;
- c) For $ii = 1:t$, calculate the gas flow redundancy of gas storage m at time ii . $\Delta Q_{gs}(ii) = \min\{Q_{gs,m}^{max} - Q_{gs,m}(ii), V_m^{max} - V_{gs,m}(ii)\}$. If the gas node where the gas storage m is connected with P2G, $\Delta Q_{P2G}(ii) = Q_{P2G}^{max} - Q_{P2G}(ii)$, the effective redundancy $\Delta Q(ii) = \min\{\Delta Q_{gs}(ii), \Delta Q_{P2G}(ii)\}$; else, $\Delta Q(ii) = \Delta Q_{gs}(ii)$. Then, arrange ΔQ in descending order;
- d) According to the descending order, $Q_{P2G}(ii)$ and $Q_{gs,m}(ii)$ are adjusted successively until $V_m(t) \geq V_m^{min}$;
- e) Update $V_m(t)$;
- f) If $V_m(t) \geq V_m^{max}$, calculate $\Delta V = V_m(t) - V_m^{max}$;
- g) For $ii = 1:t$, calculate the gas flow redundancy of gas storage m at time ii . $\Delta Q_{gs}(ii) = \min\{Q_{gs,m}(ii) - Q_{gs,m}^{min}, V_{gs,m}(ii) - V_m^{min}\}$. If the gas node where the gas storage m is connected with P2G, $\Delta Q_{P2G}(ii) = Q_{P2G}(ii) - Q_{P2G}^{min}$, the effective redundancy $\Delta Q(ii) = \min\{\Delta Q_{gs}(ii), \Delta Q_{P2G}(ii)\}$; else, $\Delta Q(ii) = \Delta Q_{gs}(ii)$. Then, arrange ΔQ in descending order;
- h) According to the descending order, $Q_{P2G}(ii)$ and $Q_{gs,m}(ii)$ are adjusted successively until $V_m(t) \leq V_m^{max}$;
- i) Update $V_m(t)$.

3. Case Studies Application

3.1. Description of Case Studies

The hybrid electricity-natural gas energy systems shown in Figure 3 are composed by the revised IEEE 39-bus power system [35] and Belgian high-calorific 20-node gas system [3]. The IEEE 39-bus power network has 46 branches, five coal-fired units, three gas-fired units and two wind power units, where the capacity of wind power units accounts for 35% of the total installed capacity of 3903 MW. The Belgian high-calorific 20-node gas system has 24 pipelines, two gas wells, three gas storages and two compressors. The parameters of the power system are from References [35,40] and the parameters of natural gas system are from Reference [3]. The revised parameters are shown in Tables 1 and 2 (inflow of gas storage is positive and outflow of gas storage is negative). Gas pressure limits of gas nodes are given in Table 3. Power demand and gas demand are given in Table 4. In addition, the theoretical predicted wind power output is given in Figure 4. The efficiency of P2G process is taken as 64% [6]. Wind curtailment cost is set as \$100/MWh [47]. The short-term optimal dispatch for this hybrid energy system is studied to illustrate the behavior of the proposed model, the adopted algorithm and the proposed constraints handling methods in several case studies. These case studies are simulated with a low level of initial line pack (0.5 Mm³). In addition, all the case studies are implemented using MATLAB language programming.

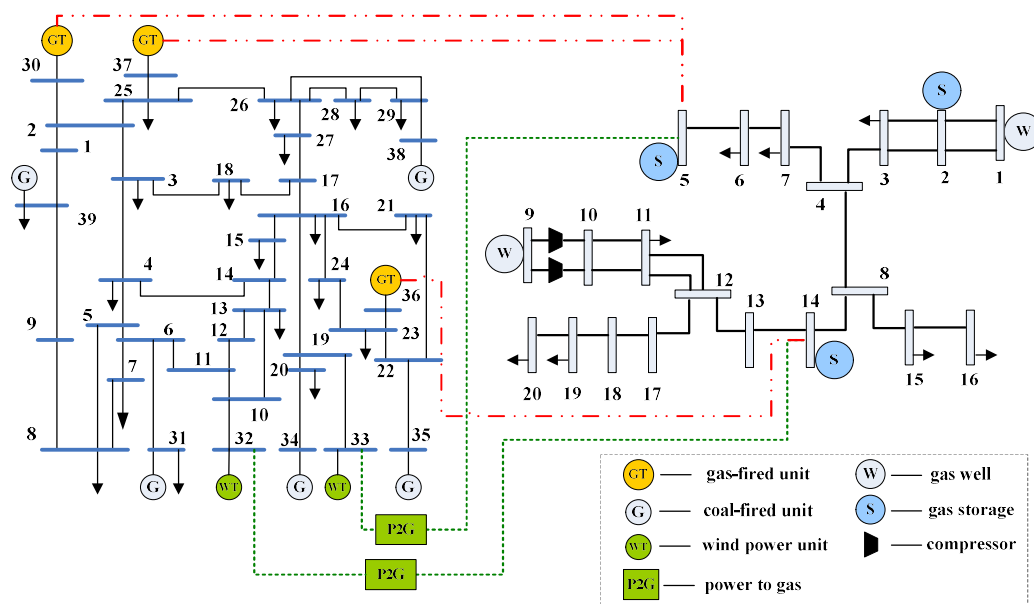


Figure 3. The hybrid electricity-natural gas energy systems.

Table 1. Parameters of power units.

Power Units	P_{max}/MW	P_{min}/MW	Ramp Up Rate/MW/h	Ramp Down Rate/MW/h
Coal-fired unit 1	470	150	80	80
Coal-fired unit 2	470	135	80	80
Coal-fired unit 3	340	73	80	80
Coal-fired unit 4	300	60	50	50
Coal-fired unit 5	243	73	50	50
Gas-fired unit 1	260	0	260	260
Gas-fired unit 2	230	0	230	230
Gas-fired unit 3	220	0	220	220
Wind power unit 1	750	0	750	750
Wind power unit 2	620	0	620	620

Table 2. Parameters of gas storage.

Gas Storage No.	Initial Capacity/Mm ³	Max Capacity/Mm ³	Min Capacity/Mm ³	Max Gas Flow/Mm ³ /h	Min Gas Flow/Mm ³ /h
Gas Storage 1	1.5	3.5	0	0.35	-0.20
Gas Storage 2	2.0	4.5	0	0.45	-0.25
Gas Storage 3	1.5	3.5	0	0.35	-0.25

Table 3. Gas pressure limits of gas nodes.

Node No.	1	2	3	4	5	6	7	8	9	10	11	12	13	14	15	16	17	18	19	20
M_{min}/bar	30	30	30	30	10	10	30	30	50	50	30	30	30	30	15	15	25	25	15	15
M_{max}/bar	100	100	100	80	80	80	80	70	70	77	70	70	70	70	70	70	70	70	70	70

Table 4. Power demand and gas demand.

Time/h	1	2	3	4	5	6	7	8	9	10	11	12
Power demand/MW/h	1272	1188	1104	960	1080	1320	1476	1584	1740	1776	1800	1860
Gas demand/Mm ³ /h	1.03	0.97	0.92	0.98	0.99	1.03	1.23	1.45	1.79	1.83	1.74	1.61
Time/h	13	14	15	16	17	18	19	20	21	22	23	24
Power demand/MW/h	1680	1560	1320	1104	1416	1680	1800	2040	1860	1632	1344	1116
Gas demand/Mm ³ /h	1.46	1.42	1.39	1.38	1.39	1.30	1.26	1.19	1.15	1.15	1.12	0.97

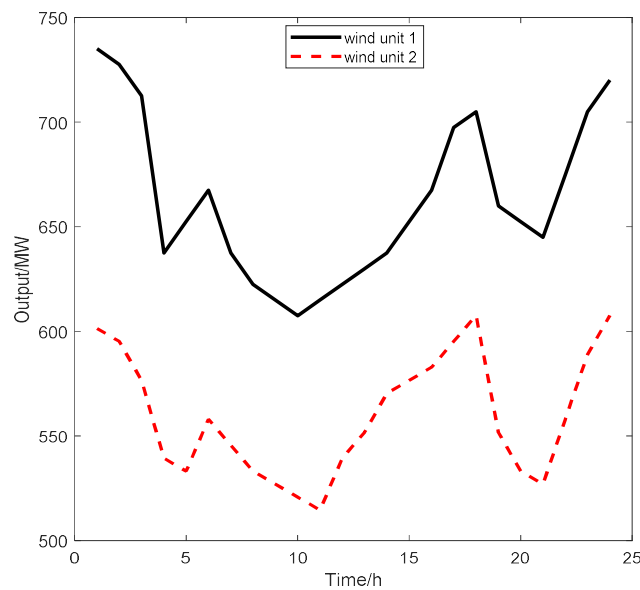


Figure 4. Predicted output of wind power units.

3.2. Analysis of Simulation Results

The Newton-Raphson method is used to obtain the power flow. Trust region method and L-M method are used to solve the non-linear equations to obtain the gas flow in natural-gas system, respectively. Furthermore, MOBHPSO [39–42] is used to optimize the multi-objective dispatch problem of hybrid electricity-natural gas energy systems based on the established models (1–3,7,12), the proposed flow chart (Figure 2), and the proposed constraints handling methods. The optimization results are shown in Tables 5 and 6. All the constraints are satisfied. The comparisons of power output and gas flow among different case studies are given in Figures 5 and 6, respectively. Moreover, it can be found the different performance of trust region method and L-M method from Figure 7 and Table 6. The wind power absorbed by P2G and the gas flow of P2G are shown in Figure 8. The volume of gas storages is given in Figure 9. The gas pressure of each gas node can be found in Appendix A.

From the obtained results, it can be seen that power output, gas flow of gas wells, gas flow of P2G, gas flow of gas storages, volume of gas storages, and gas pressure of gas nodes all satisfy their respective upper and lower bound constraints. Besides, the nodal gas flow balance equation is satisfied. Moreover, power demand and power supply are balanced which can be drawn from the calculated load loss rate $L_p = 6.37 \times 10^{-18}$. Then, the above results show that all the constraints are satisfied using the proposed constraints handling methods.

Table 5. Optimization results of the power system.

Case Studies	Fuel Cost (M\$)	SO _x Emission (ton)
Without P2G	1.080	38.193
With P2G	1.084	37.939

Table 6. Optimization results of the natural-gas system.

Case Studies	Methods	Cost of Natural-Gas/M\$	CO ₂ Emission/10 ⁴ ton	Rate of Abandoned Wind Power	Operation Cost of P2G/M\$	Absorbed CO ₂ by the Methanation Process/10 ⁴ ton	Increased Wind Power by P2G/MWh
Without P2G	Trust Region	0.741	5.791	24.85%	0	0	0
	L-M	0.695	5.790	24.85%	0	0	0
With P2G	Trust Region	0.732	5.727	6.71%	0.106	0.056	5321.66
	L-M	0.685	5.491	4.04%	0.122	0.064	6104.48

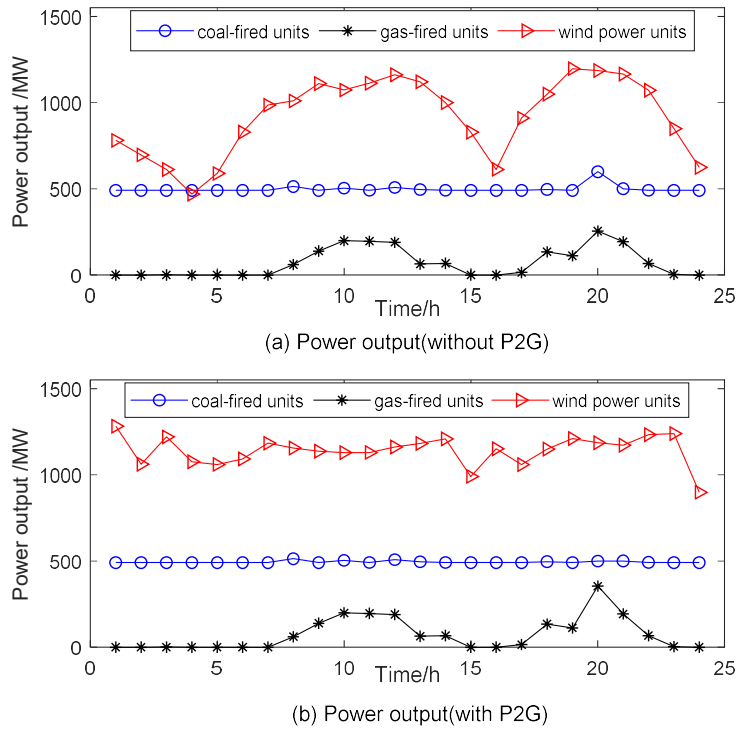


Figure 5. Comparison of power output without P2G and with P2G.

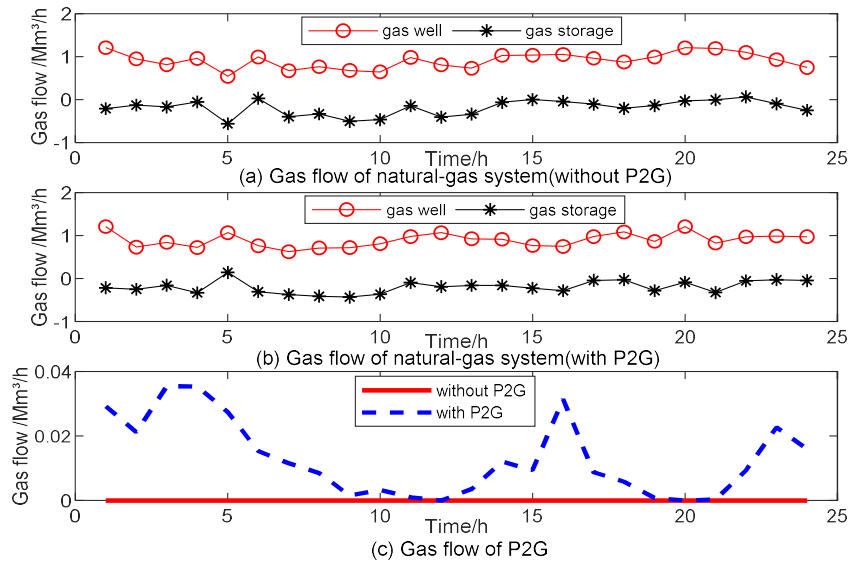


Figure 6. Comparison of gas flow without P2G and with P2G.

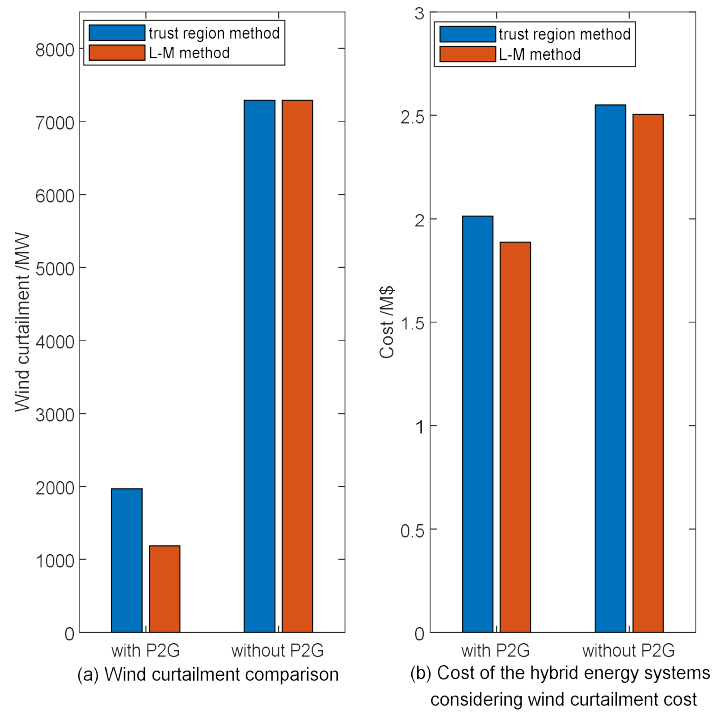


Figure 7. Results comparison of trust region method and L-M method.

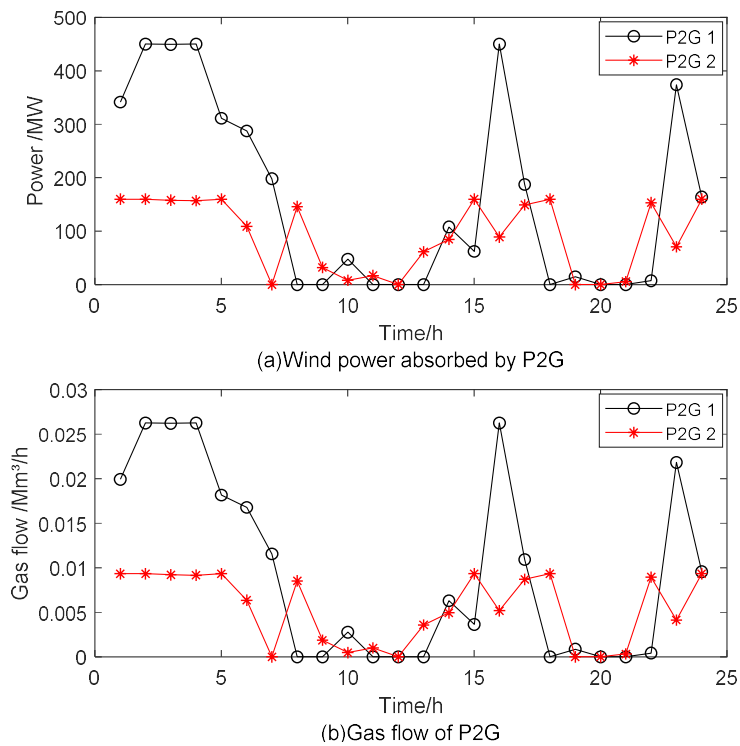


Figure 8. Wind power absorbed by P2G and the gas flow of P2G.

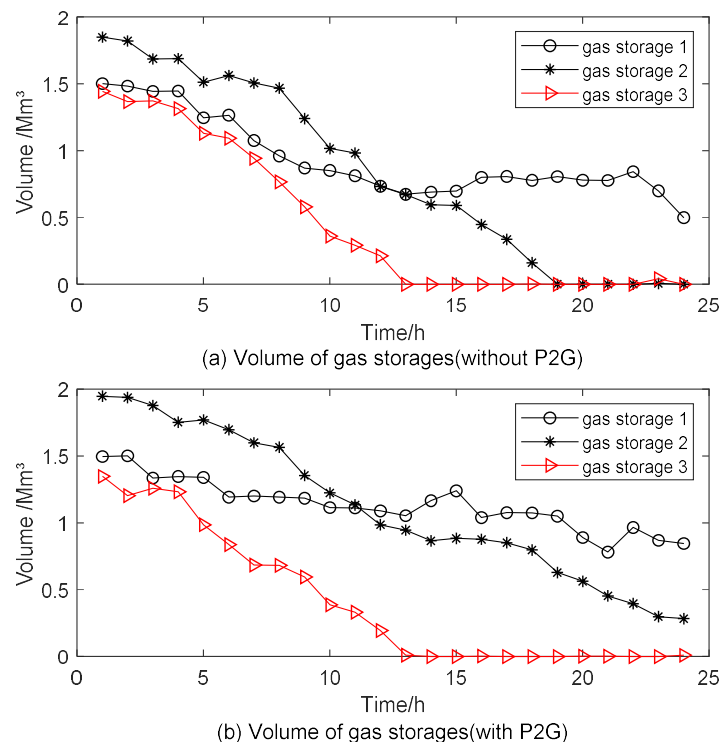


Figure 9. Volume of gas storages without P2G and with P2G.

3.2.1. Effects of P2G on the Power System

(1) From Table 5 and Figure 5, it can be seen that the fuel cost of power system with P2G is a little higher than that without P2G. At hour 20, owing to the gas injection from P2G, the pipeline pressure is higher than the maximum value, so the ‘gas demand management strategy’ is used and needs to increase the gas demand by increasing the output of gas-fired units connected with gas node 5 and 14. Then, to guarantee the power load balance, the output of coal-fired units would be reduced. Because the fuel cost of gas-fired units is higher than that of coal-fired units and the SO_x emissions of gas-fired units are lower than that of coal-fired units, it leads to increase of fuel cost and decline of SO_x emissions. The SO_x emissions are reduced by 0.254 ton. In addition, from Figure 8, most abandoned wind power can be absorbed by P2G. During hours 3–5, P2G works at its maximum value when the abandoned wind power is over the maximum capacity of P2G. Owing to the P2G, the wind power output is much smoother and so is the output of coal-fired units, which is propitious to the stability and reliability of the power system.

(2) From Table 6 and Figure 7a, it is obvious that the rate of abandoned wind power is declined from 24.85% to 6.71% (trust region) and from 24.85% to 4.04% (L-M), respectively; The wind power output is increased by 5321.66MWh (trust region) and 6104.48MWh (L-M), respectively.

3.2.2. Effects of P2G on the Natural-gas System

From Figures 6 and 9, it is obvious that the gas flow of gas wells and gas storages is lower when P2G is considered. In addition, the volume of gas storages with P2G is much larger than that without P2G. This is because the economic, clean, and low-carbon energy converted by P2G from wind power has the priority of use compared with that from natural gas network, which creates considerable economic and environmental benefits for the integrated energy systems. The cost benefit of P2G is evaluated in terms of the natural gas cost which it displaces. From Table 6, it can be seen the gas cost is reduced by \$9000 (trust region) and \$10,000 (L-M), respectively; Moreover, the environmental benefit of P2G in terms of CO_2 reduction and CO_2 absorbed in the P2G methanation process is measured. The total CO_2 emissions are declined by 1200 tons (trust region) and 3630 tons (L-M), respectively.

3.2.3. Total Cost Reduction of the Hybrid Energy Systems

The total cost of the hybrid electricity-natural gas energy systems including the wind power curtailment cost is reduced by $\$5.372 \times 10^5$ (trust region) and $\$6.165 \times 10^5$ (L-M), which can be seen from Figure 7b.

It can be concluded that the proposed model shows that the proposed constraints handling methods are effective and the feasibility of MOBHPSO algorithm for solving the multi-objective optimal dispatch problem of the hybrid electricity-natural gas energy systems is indicated. Moreover, the trust region method and L-M method are effective to solve the non-linear gas flow problem. It also can be seen that the results obtained from L-M method is much better than those obtained from trust region method.

4. Conclusions

This paper presented a multi-objective optimal dispatch model of the hybrid electricity-natural gas energy systems coupled by P2G and gas turbines in order to achieve the maximum of low-carbon economic environmental benefits. The proposed model provides not only enhanced flexibility, as it easily handles bidirectional energy flow and guarantees global optimality, but also considers the compressibility of gas, line pack of pipelines among other complicated system characteristics. The non-linear and non-convex functions of gas flow model are addressed by trust region method and L-M method. The L-M method has much better performance, which can be drawn from the simulation results. Moreover, the case studies simulation results show the feasibility of MOBHPSO algorithm for solving the multi-objective optimal dispatch problem of the hybrid electricity-natural gas energy systems and the effectiveness of proposed constraints handling methods. The obtained results also illustrate that P2G can significantly benefit the operation of both power system and natural gas system in smoothing power output, cutting down gas cost, reducing CO₂ emissions and SO_x emissions as well as avoiding wind curtailment. More specifically, the gas cost is cut down up to \$10,000, the total CO₂ emissions are declined up to 3630 tons and the SO_x emissions are reduced by 0.254 ton as well as the wind power curtailment is decreased up to 6104.48 MWh with the rate of abandoned wind power declined from 24.85% to 4.04%. Besides, the total cost including wind power curtailment cost is reduced up to $\$6.165 \times 10^5$.

Author Contributions: J.L. proposed the optimization model and algorithms, carried out case studies, completed the entire analysis, wrote and revised this paper; G.P.H. gave essential and important advice on the model of natural-gas system; W.S. gave some important suggestions on the calculation of gas flow and revised this paper.

Funding: This research was part funded by EPSRC through the Hydrogen's Value in the Energy System project, grant number EP/L018284/1 and the National Centre for Energy Systems Integration, grant number EP/P001173/1.

Acknowledgments: The authors would like to thank the financial support of the China Scholarship Council (CSC), as well as Carlos M. Correa-Posada who provided some important data used for the case studies.

Conflicts of Interest: The authors declare no conflict of interest.

Appendix A

Table A1. Gas pressure of each gas node.

Node No.	1	2	3	4	5	6	7	8	9	10
Hour 1	74.7469	73.8385	72.5356	56.7444	45.5189	41.0362	42.8709	43.8394	55.7467	61.3213
Hour 2	67.0635	66.5001	65.6495	55.1170	39.9237	38.1803	40.9818	45.8246	50.2401	55.2641
Hour 3	70.9782	70.6287	69.6258	56.8556	53.1330	46.9431	47.4426	40.3510	54.5096	59.9605
Hour 4	67.7032	67.1715	66.3961	57.2499	70.7133	54.9508	54.2037	42.9448	53.3986	58.7385
Hour 5	60.3126	59.8906	59.2212	51.7346	33.9220	33.5808	37.1390	46.9318	49.9918	54.9910
Hour 6	60.2348	60.0091	59.2823	51.2112	48.2071	40.7850	41.2236	44.1951	50.0255	55.0280
Hour 7	61.7065	61.2190	60.5111	52.7660	56.6407	46.2672	46.2665	44.8522	51.1059	56.2164
Hour 8	72.0210	71.2920	70.1714	55.5450	30.7629	30.7596	37.3143	40.5826	50.3482	55.3830

Table A1. Cont.

Node No.	1	2	3	4	5	6	7	8	9	10
Hour 9	59.6538	59.2193	58.5192	50.4304	63.6206	46.3675	45.9280	38.7845	52.4694	57.7163
Hour 10	63.8376	63.4229	62.5894	52.8985	40.6647	38.5312	40.3515	45.1444	53.4969	58.8466
Hour 11	70.6866	69.9749	68.8971	54.9136	27.6230	27.5911	35.2202	41.7990	50.9478	56.0425
Hour 12	68.9173	68.3366	67.3818	55.2606	41.9605	38.5358	40.9826	43.4697	52.3659	57.6024
Hour 13	64.6456	64.1633	63.3132	52.9436	32.3582	31.5162	36.1046	44.7830	50.4011	55.4412
Hour 14	68.1243	67.1946	66.2050	53.6897	45.2849	40.2787	41.5617	39.2924	51.8961	57.0857
Hour 15	77.3472	76.3396	75.1040	58.2513	28.6262	28.7076	37.7480	40.5386	50.1422	55.1564
Hour 16	74.0179	73.6698	72.5552	57.3796	36.5834	35.4363	40.2615	40.3234	50.9462	56.0408
Hour 17	72.7026	71.9010	70.8103	56.1345	35.5315	34.6661	39.3576	39.7726	50.2135	55.2349
Hour 18	75.1341	74.3651	73.1955	57.2444	37.5240	36.4759	40.8464	38.1481	50.2537	55.2791
Hour 19	70.4893	69.9243	68.9806	56.8986	63.1603	51.1618	51.1398	38.1952	53.7179	59.0897
Hour 20	90.0790	89.4097	87.8955	66.0627	30.6166	32.7061	44.5817	38.5313	51.2693	56.3962
Hour 21	72.9250	72.4852	71.4642	57.2781	44.5136	41.6715	44.0290	38.2162	56.4074	62.0482
Hour 22	69.5078	68.3668	67.3470	53.8900	37.1964	35.8036	39.0643	38.5332	54.3579	59.7937
Hour 23	70.0484	69.6090	68.6537	56.6512	59.8959	49.6890	49.7032	40.4218	53.2979	58.6277
Hour 24	56.7456	56.3199	55.5790	46.7811	33.0590	31.2034	33.3676	38.3445	64.6311	71.0942
Node No.	11	12	13	14	15	16	17	18	19	20
Hour 1	54.1081	50.5855	46.0875	44.7456	35.3047	25.7453	49.7105	35.4170	26.1208	25.9488
Hour 2	51.7236	50.3445	47.8200	46.7134	37.8536	29.1582	49.9537	40.2191	31.2779	31.1271
Hour 3	54.3675	51.3623	45.1763	40.7143	31.6600	21.1181	51.0356	43.0089	35.4623	35.3304
Hour 4	53.8731	51.4255	46.4733	43.5065	34.3087	24.3816	51.1668	44.6069	37.9960	37.8745
Hour 5	51.9467	50.9341	49.0610	48.4082	39.0532	30.5918	50.7221	45.1699	39.1410	39.0242
Hour 6	51.3066	49.8506	46.9020	45.3095	36.2103	27.2829	49.6736	44.8413	39.1515	39.0360
Hour 7	52.2445	50.6172	47.4860	45.9142	36.8016	27.8913	50.4070	45.1037	39.3228	39.2076
Hour 8	50.8360	48.7091	44.1013	41.0575	31.8666	21.3437	48.5566	44.1770	38.6343	38.5179
Hour 9	52.3018	49.4738	43.5577	39.5966	29.3700	17.2155	49.2713	44.1255	38.3480	38.2301
Hour 10	54.3000	52.1931	48.2816	46.3746	36.7013	27.3680	51.9234	45.6230	39.5052	39.3897
Hour 11	51.6829	49.6546	45.2476	42.3900	33.2849	23.2977	49.4998	44.9943	39.3993	39.2845
Hour 12	52.9842	50.8287	46.5780	44.1992	35.0247	25.4320	50.6144	45.2823	39.5316	39.4170
Hour 13	51.7051	50.2120	47.2589	45.8176	36.6459	27.6235	50.0282	45.1247	39.4647	39.3501
Hour 14	51.9730	49.3827	43.7844	39.8147	30.3185	19.0701	49.2116	44.5565	38.9702	38.8546
Hour 15	50.5211	48.3266	43.7034	40.9399	31.3684	20.1573	48.1649	43.6773	38.0939	37.9760
Hour 16	51.1041	48.7023	43.7603	40.7302	31.1775	19.9426	48.5071	43.4549	37.6395	37.5197
Hour 17	50.4220	48.1032	43.2388	40.2295	30.5039	18.9170	47.9215	43.0252	37.1790	37.0577
Hour 18	50.1500	47.5764	42.0906	38.4792	28.4809	15.5972	47.3952	42.5038	36.6134	36.4903
Hour 19	53.1562	49.8808	43.1425	38.5692	28.3725	15.1925	49.6243	43.5000	37.2428	37.1207
Hour 20	51.1983	48.4743	42.5615	38.5943	28.7701	15.8577	48.2927	43.2795	37.3198	37.1984
Hour 21	55.6171	51.8483	44.0882	38.5362	28.4171	15.2929	51.5608	44.9563	38.6616	38.5433
Hour 22	54.1611	50.9718	44.0340	39.1087	28.7767	15.8746	50.7701	45.4186	39.5082	39.3929
Hour 23	53.3906	50.6155	44.7480	40.9330	31.0949	19.5983	50.4247	45.3936	39.6974	39.5833
Hour 24	63.3091	58.1787	47.7707	39.5037	28.7623	16.1240	57.7734	49.4686	43.0386	42.9313

References

- Mazza, A.; Bompard, E.; Chicco, G. Application of power to gas technologies in emerging electrical systems. *Renew. Sustain. Energy Rev.* **2018**, *92*, 794–806. [\[CrossRef\]](#)
- Hibbard, P.J.; Schatzki, T. The interdependence of electricity and natural gas: Current factors and future prospects. *Electr. J.* **2012**, *25*, 6–17. [\[CrossRef\]](#)
- Correa-Posada, C.M.; Sánchez-Martín, P. Integrated power and natural gas model for energy adequacy in short-term operation. *IEEE Trans. Power Syst.* **2015**, *30*, 3347–3355. [\[CrossRef\]](#)
- Schiebahn, S.; Grube, T.; Robinius, M.; Tietze, V.; Kumar, B.; Stolten, D. Power to gas: Technological overview, systems analysis and economic assessment for a case study in Germany. *Int. J. Hydrogen Energy* **2015**, *40*, 4285–4294. [\[CrossRef\]](#)
- Götz, M.; Lefebvre, J.; Mörs, F.; McDaniel Koch, A.; Graf, F.; Bajohr, S.; Reimert, R.; Kolb, T. Renewable power-to-gas: A technological and economic review. *Renew. Energy* **2016**, *85*, 1371–1390. [\[CrossRef\]](#)
- Maroufmashat, A.; Fowler, M. Transition of future energy system infrastructure: Through power-to-gas pathways. *Energies* **2017**, *10*, 1089. [\[CrossRef\]](#)

7. Mukherjee, U.; Maroufmashat, A.; Narayan, A.; Elkamel, A.; Fowler, M. A stochastic programming approach for the planning and operation of a power to gas energy hub with multiple energy recovery pathways. *Energies* **2017**, *10*, 868. [[CrossRef](#)]
8. Eveloy, V.; Gebreegziabher, T. A review of projected power-to-gas deployment scenarios. *Energies* **2018**, *11*, 1824. [[CrossRef](#)]
9. Clegg, S.; Mancarella, P. Integrated modeling and assessment of the operational impact of power-to-gas (P2G) on electrical and gas transmission networks. *IEEE Trans. Sustain. Energy* **2015**, *6*, 1234–1244. [[CrossRef](#)]
10. Department of Energy and Climate Change. *The Future of Heating: Meeting the Challenge*; HM Government: London, UK, 2013.
11. Ball, M.B.; Wietschel, M. *The Hydrogen Economy: Opportunities and Challenges*; Cambridge University Press: Cambridge, UK, 2009.
12. An, S.; Li, Q.; Gedra, T.W. Natural gas and electricity optimal power flow. In Proceedings of the IEEE PES Transmission and Distribution Conference and Exposition, Dallas, TX, USA, 7–12 September 2003. [[CrossRef](#)]
13. Chen, S.; Wei, Z.N.; Sun, G.Q.; Wang, D.; Sun, Y.H.; Zang, H.X.; Zhu, Y. Probabilistic energy flow analysis in integrated electricity and natural-gas energy systems. *Proc. CSEE* **2015**, *35*, 6331–6340. [[CrossRef](#)]
14. Sun, G.Q.; Chen, S.; Wei, Z.N.; Chen, S.; Li, Y.C. Probabilistic optimal power flow of combined natural gas and electric system considering correlation. *Autom. Electr. Power Syst.* **2015**, *39*, 11–17. [[CrossRef](#)]
15. Osiadacz, A.J. *Simulation and Analysis of Gas Networks*; Gulf Publishing Company: Houston, TX, USA, 1987.
16. Liu, C.; Shahidehpour, M.; Fu, Y.; Li, Z.Y. Security-constrained unit commitment with natural gas transmission constraints. *IEEE Trans. Power Syst.* **2009**, *24*, 1523–1536. [[CrossRef](#)]
17. Geidl, M.; Andersson, Q. Optimal power flow of multiple energy carriers. *IEEE Trans. Power Syst.* **2007**, *22*, 145–155. [[CrossRef](#)]
18. Qadrdan, M.; Wu, J.Z.; Jenkins, N.; Ekanayake, J. Operating strategies for a GB integrated gas and electricity network considering the uncertainty in wind power forecasts. *IEEE Trans. Sustain. Energy* **2014**, *5*, 128–138. [[CrossRef](#)]
19. Chaudry, M.; Jenkins, N.; Strbac, G. Multi-time period combined gas and electricity network optimization. *Electr. Power Syst. Res.* **2008**, *78*, 1265–1279. [[CrossRef](#)]
20. Wang, W.L.; Wang, D.; Jia, H.J.; Chen, Z.Y.; Guo, B.Q.; Zhou, H.M.; Fan, M.H. Steady state analysis of electricity-gas regional integrated energy system with consideration of NGS network status. *Proc. CSEE* **2017**, *37*, 1293–1304. [[CrossRef](#)]
21. Odetayo, B.; Kazemi, M.; MacCormack, J.; Rosehart, W.D.; Zareipour, H.; Seifi, A.R. A chance constrained programming approach to the integrated planning of electric power generation, natural gas network and storage. *IEEE Trans. Power Syst.* **2018**, *33*, 6883–6893. [[CrossRef](#)]
22. Guandalini, G.; Robinius, M.; Grube, T.; Campanari, S.; Stolten, D. Long-term power-to-gas potential from wind and solar power: A country analysis for Italy. *Int. J. Hydrogen Energy* **2017**, *42*, 13389–13406. [[CrossRef](#)]
23. Liu, W.J.; Wen, F.S.; Xue, Y.S. Power-to-gas technology in energy systems: Current status and prospects of potential operation strategies. *J. Mod. Power Syst. Clean Energy* **2017**, *5*, 439–450. [[CrossRef](#)]
24. He, L.C.; Lu, Z.G.; Zhang, J.F.; Geng, L.J.; Zhao, H.; Li, X.P. Low-carbon economic dispatch for electricity and natural gas systems considering carbon capture systems and power-to-gas. *Appl. Energy* **2018**, *224*, 357–370. [[CrossRef](#)]
25. International Energy Agency. *Prospects for Hydrogen and Fuel Cell*; International Energy Agency: Paris, France, 2005.
26. De Vries, H.; Florisson, O.; Tiekstra, G. Safe operation of natural gas appliances fueled with hydrogen/natural gas mixtures (progress obtained in the naturally-project). In Proceedings of the International Conference on Hydrogen Safety, San Sebastián, Spain, 11–13 September 2007. [[CrossRef](#)]
27. Dodds, P.E.; Demoullin, S. Conversion of the UK gas system to transport hydrogen. *Int. J. Hydrogen Energy* **2013**, *38*, 7189–7200. [[CrossRef](#)]
28. Biegger, P.; Kirchbacher, F.; Medved, A.R.; Miltner, M.; Lehner, M.; Harasek, M. Development of honeycomb methanation catalyst and its application in power to gas systems. *Energies* **2018**, *11*, 1679. [[CrossRef](#)]
29. Li, Y.; Liu, W.J.; Zhao, J.H.; Wen, F.S.; Dong, C.Y.; Zheng, Y.; Zhang, R. Optimal dispatch of combined electricity-gas-heat energy systems with power-to-gas devices and benefit analysis of wind power accommodation. *Power Syst. Technol.* **2016**, *40*, 3680–3688. [[CrossRef](#)]

30. Clegg, S.; Mancarella, P. Integrated electrical gas network flexibility assessment in low-carbon multi-energy systems. *IEEE Trans. Sustain. Energy* **2016**, *7*, 718–731. [[CrossRef](#)]
31. Ye, J.; Yuan, R.X. Integrated natural gas, heat, and power dispatch considering wind power and power-to-gas. *Sustainability* **2017**, *9*, 602. [[CrossRef](#)]
32. Li, G.Q.; Zhang, R.F.; Jiang, T. security-constrained bi-level economic dispatch model for integrated natural gas and electricity systems considering wind power and power-to-gas process. *Appl. Energy* **2017**, *194*, 696–704. [[CrossRef](#)]
33. Guandalini, G.; Campanari, S.; Romano, M.C. Power-to-gas plants and gas turbines for improved wind energy dispatchability: Energy and economic assessment. *Appl. Energy* **2015**, *147*, 117–130. [[CrossRef](#)]
34. Chen, Z.Y.; Wang, D.; Jia, H.J.; Wang, W.L.; Guo, B.Q.; Qu, B.; Fan, M.H. Research on optimal day-ahead economic dispatching strategy for microgrid considering P2G and multi-source energy storage system. *Proc. CSEE* **2017**, *37*, 3067–3077. [[CrossRef](#)]
35. Wei, Z.N.; Zhang, S.D.; Sun, G.Q.; Zang, H.Y.; Chen, S.; Chen, S. Power-to-gas considered peak load shifting research for integrated electricity and natural-gas energy systems. *Proc. CSEE* **2017**, *37*, 4601–4609. [[CrossRef](#)]
36. He, C.; Liu, T.Q.; Wu, L.; Shahidepour, M. Robust coordination of interdependent electricity and natural gas systems in day-ahead scheduling for facilitating volatile renewable generations via power-to-gas technology. *J. Mod. Power Syst. Clean Energy* **2017**, *5*, 375–388. [[CrossRef](#)]
37. Shu, K.G.; Ai, X.M.; Fang, J.K.; Yao, W.; Chen, Z.; He, H.B.; Wen, J.Y. Real-time subsidy based robust scheduling of the integrated power and gas system. *Appl. Energy* **2019**, *236*, 1158–1167. [[CrossRef](#)]
38. Qu, K.P.; Zheng, B.M.; Yu, T.; Li, H.F. Convex decoupled-synergetic strategies for robust multi-objective power and gas flow considering power to gas. *Energy* **2019**, *168*, 753–771. [[CrossRef](#)]
39. Liu, J.; Luo, X.J. Environmental economic dispatching adopting multi-objective random black-hole particle swarm optimization algorithm. *Proc. CSEE* **2010**, *30*, 105–111. [[CrossRef](#)]
40. Liu, J.; Luo, X.J. Short-term optimal environmental economic hydrothermal scheduling based on handling complicated constraints of multi-chain cascaded hydropower station. *Proc. CSEE* **2012**, *32*, 27–35. [[CrossRef](#)]
41. Liu, J.; Luo, X.J. Optimal economic emission hydrothermal scheduling using a novel algorithm based on black hole theory and annual profit analysis considering fuel gas desulphurization. In Proceedings of the 1st International IET Renewable Power Generation Conference, Edinburgh, UK, 6–8 September 2011. [[CrossRef](#)]
42. Liu, J.; Lu, Q.W.; Liu, Y. Optimal capacity allocation of hybrid wind-solar-battery power system containing electric vehicles. In Proceedings of the 5th International IET Renewable Power Generation Conference, London, UK, 21–22 September 2016.
43. Byrd, R.H.; Gilbert, J.C.; Nocedal, J. A trust region method based on interior point techniques for nonlinear programming. *Math. Program.* **2000**, *89*, 149–185. [[CrossRef](#)]
44. Mohamed Abdelmageed Abdelaziz, M.; Farag, H.E.; El-Saadany, E.F.; Mohamed, Y.A.I. A novel and generalized three-phase power flow algorithm for islanded microgrids using a newton trust region method. *IEEE Trans. Power Syst.* **2013**, *28*, 190–201. [[CrossRef](#)]
45. Wilamowski, B.M.; Yu, H. Improved computation for Levenberg-Marquardt training. *IEEE Trans. Neural Netw.* **2010**, *21*, 930–937. [[CrossRef](#)]
46. Kanzowa, C.; Yamashita, N.; Fukushima, M. Levenberg-Marquardt methods with strong local convergence properties for solving nonlinear equations with convex constraints. *J. Comput. Appl. Math.* **2004**, *172*, 375–397. [[CrossRef](#)]
47. Zheng, J.; Wen, F.S.; Li, L.; Wang, K.; Gao, C. Transmission system expansion planning considering combined operation of wind farms and energy storage systems. *Autom. Electr. Power Syst.* **2013**, *37*, 135–142. [[CrossRef](#)]

